Assessment of modeling methods for predicting load resulting from hydrogen-air detonation

Di Chen, Chengqing Wu, Jun Li

School of Civil and Environmental Engineering, University of Technology Sydney, Sydney, NSW, 2007, Australia

Corresponding author: Chengqing Wu (chengqing.wu@uts.edu.au)

Keywords: Hydrogen detonation, load prediction, modelling, fluid-chemistry-structural coupling, multi-material ALE

Abstract: As hydrogen becomes an increasingly vital component in the transition toward a sustainable energy system, its flammable and detonable properties necessitate a comprehensive understanding of its explosive characteristics. This study evaluated the accuracy and computational efficiency of an innovative numerical approach that integrates CESE compressible CFD solver, chemistry reaction model, and structural FEM solver within LS-DYNA to predict hydrogen detonation loads. Comparisons were made with the commonly used energy equivalent methods, i.e., the TNT equivalent method, and the high-pressure volume method, which utilizes multi-material ALE techniques. Hydrogen detonation test results from open-air space, open-air space with a blast wall, and semi-confined space were compared against numerical simulations. The results revealed that, for scaled distance exceeding 0.79 m/kg$^{1/3}$, all three methods accurately predicted the peak overpressure. The TNT equivalent method exhibited an unexpectedly high energy efficiency factor exceeding 0.51, significantly surpassing the recommended range of 0.01 to 0.1 for typical vapor cloud

accidents. The CESE-chemistry coupling method exceled in capturing overpressure duration and structural response due to its consideration of chemical kinetics. As the scaled distance reduced to 0.37 m/kg$^{1/3}$, the CESE-chemistry coupling method maintained its proficiency in modelling pressure waves, while the TNT equivalent method overestimated peak pressure by 494%. Conversely, the high-pressure volume method underestimated the peak pressures within or near the H_2-air cloud. Nevertheless, the CESE-chemistry coupling method required significantly higher computational costs, with 15 to 20 times more computational time compared to the other two methods, and 60 % to 70% of the total computation time was spent solving chemical kinetics. It is concluded from the current study that for scenarios involving close scaled distances (less than 0.37 m/kg$^{1/3}$) or where the structure locates inside or near the gas cloud, the CESE-chemistry coupling method may be preferred despite its higher computational demands. Conversely, for simulations prioritizing computational efficiency and larger scaled distances, the TNT equivalent method or high-pressure volume method is recommended. These findings offer guidelines for researchers and engineering professionals engaged in assessing and mitigating risks associated with hydrogen explosion accidents in the pursuit of safe and sustainable hydrogen utilization.

1. Introduction

Hydrogen plays a pivotal role in the global energy transformation as the world strives to limit global warming within two degrees Celsius by 2050, with a target of reducing energy-related CO_2 emissions by 60% [1]. The Hydrogen Council predicted that hydrogen would provide 18% of the final energy demand by 2050 [1]. The growing importance of hydrogen energy has led to the formulation of hydrogen energy strategies and development roadmaps by various countries and organizations worldwide, including the US [2], China [3], the European Union [4], Canada [5], Germany [6], Russia [7], Japan [8], Australia [9]. As shown in Figure 1, these

hydrogen policies highlight the strategic significance of hydrogen in supporting a nation's energy policies.

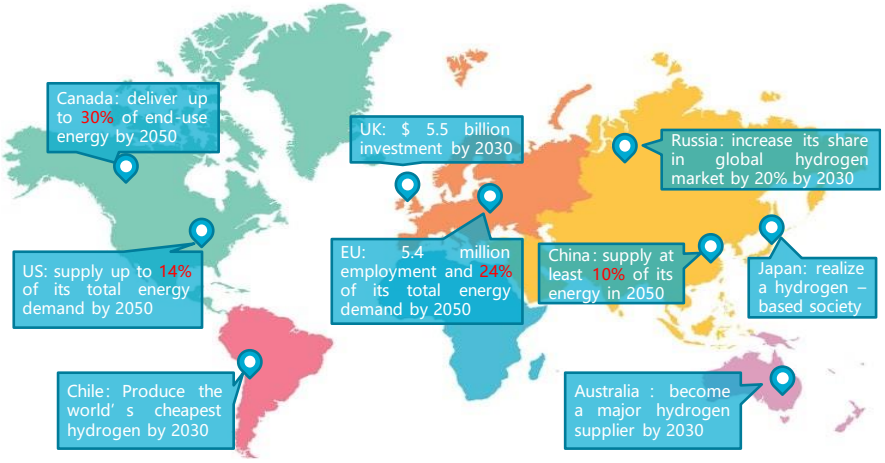

Figure 1 Hydrogen policies in major countries or organizations worldwide [2-11]

However, as listed in Table 1, while hydrogen offers immense potential as a clean energy, its significantly higher flammability and detonability as compared to methane (the primary component of natural gas) pose significant safety challenges in its production, transportation, storage, and utilization. Mishandling hydrogen can lead to extreme explosion accidents with severe consequences, including structural damages, injuries, fatalities, economic losses, and social disruption. A notable example of such an accident occurred in South Korea in 2019, resulting in six casualties and extensive damage to surrounding buildings [12]. Detonation is the most destructive form of explosion for gas explosion, given the high pressures (C-J pressure is 15.8 bar) and velocities (C-J velocity is 1971 m/s) associated with detonation waves [13].

Table 1 Comparison of hydrogen and methane related to combustion and explosion characteristics [14, 15]

Property	H_2	CH_4
Flammability range	4-75%	4.3 – 15%
Ignition energy	0.02 mJ	0.28 mJ
Minimum autoignition temperature	520	540
Laminar Flame Speed	28 m/s	3.5 m/s
Spontaneous combustion	Self-ignition would be induced if high-pressure H_2 is suddenly released	unlikely in air
Detonation level	Detonable in wide range of concentrations (18%-59%)	unlikely in air

Figure 2 Hydrogen explosion accident in South Korea on May 2019, six casualties and several surrounding buildings (up to 100 m away) were seriously damaged [12]

To design reliable blast-resistant structures, it is crucial to have comprehensive knowledge of hydrogen explosion characteristics and dynamic response prediction of structures [16]. However, accurately obtaining the temporal and spatial distribution of overpressure on structures presents a significant challenge. Experimental tests using pressure sensors can provide direct overpressure measurements [17], but they often fail to capture the full spatial and temporal overpressure distributions. Furthermore, experimental tests can be costly and pose safety concerns, rendering them less practical for engineering protection design [18].

Energy equivalent method is one of the widely used approaches for assessing blast effects. With this method, the gas explosion source was replaced by an equivalent amount of high explosive causing a comparable damage [19]. The TNT equivalent method is one of such energy equivalent methods converting gas cloud into the equivalent TNT mass [20]. Subsequently, the structural response resulting from the gas explosion is derived based on equivalent TNT detonation. For example, Kim et al. [12] employed this method to study the response of a barrier wall subjected to a hydrogen storage tank explosion. Guo et al. [12, 21] examined the neighboring pipeline response owing to gas explosions using the TNT equivalent method. Zhang et al. [22] explored the response of spherical tanks under gas

explosions based on this method. The TNT equivalent method is widely believed to be capable of predicting peak pressure for far-field explosions [16]. However, it may provide overly conservative predictions for near-field scenarios [16]. Another disadvantage for TNT equivalent method is that an energy efficiency factor needs to be determined case by case, because not all combustion energy is converted to blast load in gas explosion. For most accident scenarios, energy efficiency factor falls between 0.01 – 0.1, with a statistical average value of 0.04 [21, 23, 24], but its value for hydrogen detonation is yet to be determined.

Another commonly used energy equivalent method for simulating blast propagation from gas explosions is the high-pressure volume method. This method assumes that the combustion process occurs very rapidly in a constant volume, leading to the conversion of all the combustion energy into pressure at the beginning of the simulation. As a result, the gas cloud is represented as a cloud of gas with homogeneous high pressure that expands rapidly and interacts with its surroundings, including nearby structures. Jiang et al. [25] investigated a natural gas explosion accident in a building based in this method. They analysed the overpressure and fragments distribution resulting from the explosion. Similarly, Zhang et al. [26] simulated the dynamic response of a coal mine refuge chamber against methane-air mixture explosion using high-pressure volume method. However, this method inevitably underestimates the peak pressure within or near the fuel cloud. Detonation waves have a shock wave front where the highest pressure exists. Unfortunately, the high-pressure volume method averages the overpressure distribution inside the explosion source, thereby not fully capturing the complex shock wave phenomena in actual detonations. This method is less likely to provide overestimated predictions, and the existing material model for high explosives in commercial codes can be easily adjusted to suit different types of gas explosion sources, contributing to the widespread use of this method. Till now, high-pressure volume

method has not been found to model the structural response subjected to hydrogen detonation, hence its performance is examined in this study.

Aside from the energy equivalent methods, Computational Fluid Dynamics (CFD) methods are also commonly used to estimate hydrogen detonation loads. It should be noted that simulating the gas detonation in large-scale scenarios is not feasible due to the refined mesh requirement in large computation domain, which is on the order of micrometres [27]. As a result, simulations for hydrogen detonation are typically conducted on coarser meshes of several centimetres for large-scale scenarios [27-33]. In these simulations, either several steps of chemical reaction models or reaction progress variable were adopted to approximate the complex chemical reactions occurring during the detonation process. Commercial or open-source CFD codes, such as COM3D, Fluent, OpenFoam, have been employed in these simulations. However, these CFD tools mainly focus on the modelling of blast loads, while structures are treated as rigid.

To address the challenges of simulating structural responses subjected to gas explosions, LS-DYNA recently developed the CESE solver, Chemistry solver, and LS-DYNA finite element method (FEM) structural solver [34] which are fully coupled with one and another. The Chemistry solver is based on the finite-rate chemistry theory [35] to solve chemical kinetics. On the other hand, the CESE solver is a compressive CFD solver that relies on the space-time conservation element and solution element (CESE) theory [36]. The CESE solver offers several advantages, including a unified space-time treatment, and a simple shock capturing strategy [37]. Importantly, the CESE solver can fully couple with the LS-DYNA finite element method (FEM) structural solver. By doing so, the software becomes well- suitable for solving structural response under H_2-air detonations. The immersed boundary method (IBM)

is utilised to treat the interface between fluid and structure. In this strategy, the fluid mesh is fixed while the structure mech is moving inside the fluid mesh. The CESE solver detects the displacement and velocity of interface from the FEM solver and provides feedback pressure to the FEM solver [34]. With this approach, the fluid and structure mesh can be independent of each other[35]. IBM method proves to be robust and capable of handling large deformation problems from explosion events. The coupling strategy among the three solvers is presented in Figure 3. The CESE-chemistry coupling method has been used to simulate the metal forming by H_2-O_2 detonation [38], C_3H_8-O_2 detonation [35], aluminium tube deformation against H_2-O_2 detonation [39], and concrete wall response against H_2-air detonation [40], and good agreement with experimental data has been observed. However, this method is so time-consuming compared to energy equivalent method that it is not always feasible to perform such expensive simulation in engineering practice.

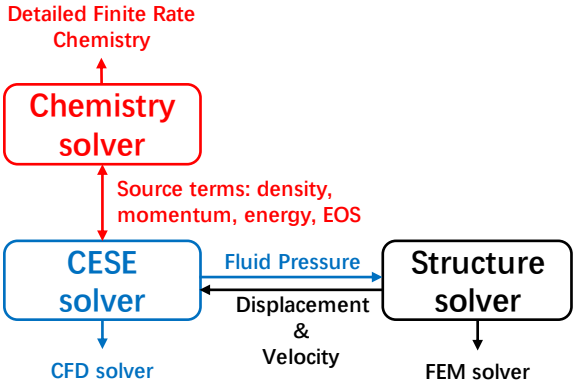

Figure 3 Coupling strategy among CESE, chemistry, and FEM solvers in LS-DYNA [34]

In this study, the accuracy and computational effectiveness of three methods, namely the CESE-chemistry coupling method, TNT equivalent method, and high-pressure volume method, for hydrogen detonation load prediction, were assessed. As the confinement has notable impact on blast loads [18, 41, 42], the experimental results from open-air space, open-air space with blast wall, and semi-confined space were compared. The results of this study facilitate the optimal selection of blast prediction methods by thoroughly evaluating their performance across diverse scenarios.

2. Methodology and numerical model

2.1. CESE-chemistry coupling method

A detailed chemical reaction was coupled with the CESE solver. The Z-22 reaction model for H_2-air combustion process, developed by Zettervall in 2018 [43], was employed to simulate the H_2-air chemical reaction in the detonation process. This model consists of 9 species and 22 individual reactions, and the detailed reactions are listed in Table 2. The computational time for the Chemistry solver is directly proportional to the square of the number of species in the reaction model [44]. Therefore, simpler reaction models with fewer species would significantly reduce the computational time. However, it is crucial to strike a balance between computational efficiency and accuracy. While overly simplified reaction models can lead to faster simulations, they may also cause convergence problems.

Table 2 Skeletal H_2-O_2 reaction mechanism, Units are mole-cm-sec-K-cal [43].

#	Reaction	A	n	E
1	H2 + O2 => H + HO2	7.40E+05	2.43	53500
2	H2 + M => H + H + M	4.57E+19	-1.4	105100
3	HO2 + H2 => H2O2 + H	3.00E+06	2	21000
4	H + O2 => OH + O	2.45E+14	0	16800
5	OH + O => H + O2	1.20E+13	0	690
6	O + H2 => OH + H	1.80E+10	1	8826
7	OH + H => O + H2	8.00E+09	1	6760
8	H2 + OH => H2O + H	1.17E+09	1.3	3626
9	H2O + H => H2 + OH	5.09E+09	1.3	18588
10	OH + OH => O + H2O	6.00E+08	1.3	0
11	O + H2O => OH + OH	5.90E+09	1.3	17029
12	H + O2 + M => HO2 + M	1.80E+18	-0.8	0
13	H + HO2 => OH + OH	1.50E+14	0	1004
14	H + HO2 => H2 + O2	2.50E+13	0	700
15	OH + HO2 => H2O + O2	2.00E+13	0	1000
16	HO2 + HO2 => H2O2 + O2	8.00E+13	0	0
17	H2O2 + M => OH + OH + M	1.30E+17	0	34500
18	OH + OH + M => H2O2 + M	9.86E+14	0	-5070
19	H2O2 + OH => H2O + HO2	1.00E+13	0	1800
20	H2O + HO2 => H2O2 + OH	2.86E+13	0	32790
21	OH + H + M => H2O + M	2.20E+22	-2	0
22	H + H + M => H2 + M	1.80E+18	-1	0

2.2. TNT equivalent method

The TNT-equivalency method is based on the energy equivalency principle, converts a gas explosion into a TNT blast using Equation 1[20]:

$$W_{\mathrm{TNT}} = \eta \frac{W_{\mathrm{H_2}} H_{\mathrm{H_2}}}{H_{\mathrm{TNT}}} \qquad \text{Equation 1}$$

where W_{TNT} indicates the equivalent weight of TNT, kg; $W_{\mathrm{H_2}}$ is the weight of hydrogen involved in the explosion, kg; $H_{\mathrm{H_2}}$ is the hydrogen combustion heat, 120 MJ/kg [40]; H_{TNT} represents the blast energy of TNT, 4.5 MJ/kg [21]; η is energy efficiency factor of the vapor cloud explosion.

Another crucial concept related to TNT explosions is the scaled distance, determined by Equation 2 [16]:

$$Z = \frac{R}{W_{\mathrm{TNT}}^{1/3}} \qquad \text{Equation 2}$$

where Z detonates scaled distance, m/kg$^{1/3}$; R represents the distance from the centre of explosive charge to the target point. The scaled distance serves as a scaling factor, enabling a comparison of blast effects from various charge weights of the same explosive at different distances. In the numerical model using TNT equivalent method, the charge centre was located at the ignition position.

The *MAT-HIGH_EXPLOSIVE_BURN material model was selected to model TNT explosions, and *EOS_JWL was used to model the equation of state for TNT. *MAT_NULL and *EOS_LINEAR_POLYNOMIAL were adopted to describe the state of ambient air. For more detailed information, the LS-DYNA User's Manual [45] contains relevant theory, and the specific parameter values are listed in Table 3.

The multi-material arbitrary Lagrangian Eulerian (MMALE) approach is well-suited for solving fluid-structural interactions involving large deformations and dynamic loading [46]. MMALE method allows the Lagrange elements (representing the structure) to independently adjust their positions within the flow mesh, while let each of the flow mesh accommodate multiple materials. In this study, the initial setup involved establishing air meshes as the background mesh. Then these meshes were filled with either TNT or high-pressure air.

Table 3 Material and EOS parameters used for air, TNT, high-pressure H_2-air, and reinforced concrete, units are kg-m-s [25, 40, 47, 48]

Ambient air	*MAT_NULL						
	Density						
	1.20						
	*EOS_LINEAR_POLYNOMIAL						
	C_4	C_5	E_0	V_0			
	0.4	0.4	2.53×10^5	1			
TNT	*MAT-HIGH_EXPLOSIVE_BURN						
	Density	Detonation velocity	P_{CJ}				
	1630	6930	2.1×10^{10}				
	*EOS_JWL						
	A	B	R_1	R_2	ω	E_0	V_0
	3.712×10^{11}	3.231×10^9	4.15	0.95	0.35	7×10^9	1
High-pressure H_2-air	*MAT-HIGH_EXPLOSIVE_BURN						
	Density	Detonation velocity	P_{CJ}				
	0.87	1969	1.60×10^6				
	*EOS_LINEAR_POLYNOMIAL						
	C_4	C_5	E_0	V_0			
	0.24	0.24	2.95×10^6	1			
Concrete	*MAT_CSCM_CONCRETE						
	Density	Compressive strength					
	2400	4.8×10^7					
Rebar	*MAT_PIECEWISE_LINEAR_PLASTICITY						
	Density	Young's modulus	Poisson's ratio	Yield strength			
	7850	2.1×10^{11}	0.27	3.4×10^8			
	*MAT_RIGID						
	DENSITY	Young's modulus	Poisson's ratio				
	7850	2.1×10^{11}	0.3				

2.3. High-pressure volume method

In the numerical study, the *MAT_HIGH_EXPLOSIVE_BURN material model was employed to simulate the high-pressure combustion product of H_2-air mixture. Additionally, *EOS_LINEAR_POLYNOMIAL was adopted as the equation of state for the combustion product, and the initial pressure is given by Equation 3:

$$P = C_0 + C_1\mu + C_2\mu^2 + C_3\mu^3 + \left(C_4 + C_5\mu + C_6\mu^2\right)E \qquad \text{Equation 3}$$

where P is pressure, E is the initial energy per unit reference volume, $\mu = \rho/\rho_0 - 1$, and ρ/ρ_0 is the ratio of initial density to reference density defined in *MAT_NULL. When Equation 3 is used to model gas, $C_0 = C_1 = C_2 = C_3 = C_6 = 0$, and $C_4 = C_5 = \gamma - 1$, where

$$\gamma = \frac{C_\mathrm{p}}{C_\mathrm{v}} \qquad \text{Equation 4}$$

is the ratio of specific heat; C_p is the constant pressure heat capacities; C_v is the constant volume heat capacities. Assuming the the high-pressure combustion product of H_2-air mixture is ideal gas, the pressure is given by Equation 5. Hence the initial pressure inside the high-pressure cloud resulting from 30% H_2-air detonation can be calculated as 0.71 MPa (absolute pressure). Detailed parameters (suitable for 30% H_2-air mixture) are listed in Table 3.

$$P = (\gamma - 1)\frac{\rho}{\rho_0}E \qquad \text{Equation 5}$$

Similarly, *MAT_NULL and *EOS_LINEAR_POLYNOMIAL were adopted to describe the state of ambient air, and the detailed parameter values can be found in Table 3.

2.4. Other constitutive models used in simulation

Three other material models were used in this study. Specifically, the *MAT_CSCM_CONCRETE and *MAT_PIECEWISE_LINEAR_PLASTICITY were utilised to model the concrete wall and rebar, and the *MAT_RIGID was employed to model the steel

blast chamber in Case 3. The detailed theory for these models can be found in LS-DYNA User's Manual [45], and the parameter values are presented in Table 3.

2.5. Numerical model

2.5.1. Case 1 – Hydrogen detonation in open-air space

A 300 m^3 H_2-air detonation was conducted in open-air space[49]. The H_2-air mixture, comprising 30% (vol) of hydrogen, was contained within a thin dome tent constructed of an aluminum frame and plastic film. The total mass of hydrogen used in the experiment was approximately 7.3 kg. A direct detonation was initiated at the bottom center of the hydrogen-air mixture using a 10 g C-4 high explosive. The dome had a height of 5.7 m, which deviated from an ideal hemisphere. However, for the numerical model utilizing high-pressure method and CESE-chemistry coupling method, the dome shape was simplified as an ideal hemisphere with a radius of 5.2 m. Figure 4 displays a visualization of the simplified dome shape, the C4 high explosive, and the locations of pressure sensors. The aluminium frame and plastic film were ignored in the modelling. Owing to the symmetric nature of the explosion source, only one quarter of the problem was modelled. Figure 5 illustrates the geometric model employed for the CESE-chemistry coupling method, with dimensions of 20 m, 6.2 m, and 6.2 m in the X, Y, and Z directions respectively. The initial volume is a highly energetic region represented as a cubic shape measuring 0.3 m × 0.3 m × 0.3 m, designed to facilitate a rapid detonation. In this region, the pressure and temperature were 0.71 MPa and 3000 K, respectively, where the pressure of 0.71 MPa was calculated by Equation 5, and the same initial conditions for the CESE-coupling method in the following two scenarios. The pressure and temperature in the rest of the computational domain were 0.1 MPa and 300 K, respectively. Within the fuel region, the mesh size was 15 mm and smoothly increaseed to 30 mm before reaching X =15.7 m. Finally, it gradually expanded to 50 mm to the boundary. The number of mesh elements was approximately 2400 × 10^4. The three outer faces of the model were defined as

nonreflective boundary, the bottom face was a reflective boundary, and the remaining two faces were considered as symmetric boundary.

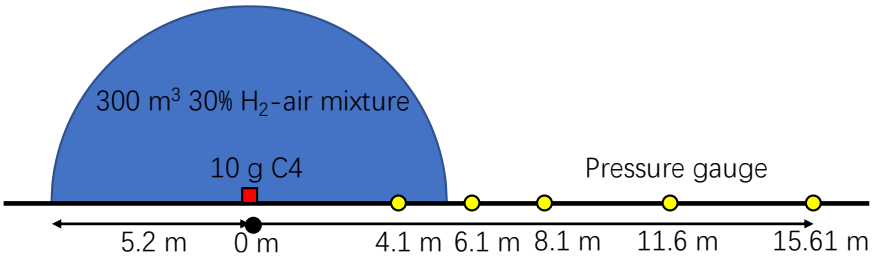

Figure 4 Experimental setups for the 300 m^3 30% H_2-air detonation test in open-air space [49]

Figure 5 Geometry model established for CESE-chemistry coupling method

In the numerical model using high-pressure volume method, there was no specific initial volume. The entire H_2-air region was replaced by a high-pressure volume. For the numerical model based on TNT equivalent method, Equation 1 was utilized to estimate the TNT equivalent mass. Initially, an energy efficiency factor of 0.04 was adopted, resulting an estimated TNT equivalent mass of 7.9 kg. However, when comparing the estimated incident pressure from the UN Saferguard website [50] at a distance of 15.61 m (a far-field measuring point, where the TNT equivalent method is supposed to be applicable), it was only 20.69 kPa, which significantly deviated from the experimental result of 91.2 kPa. According to the captured peak pressure at 15.61 m, the equivalent TNT mass was increased to 99.8 kg where the energy efficiency factor was adjusted to 0.51. The higher efficiency factor in this study can be attributed to the increased energy-yielding efficiency for homogeneous H_2-air mixture detonation. The previous range of 0.01 - 0.1, established from a statistical analysis of over 120 damage points across 23 accidents, indicated that 97% of the cases fell within this lower range (0.01 – 0.1) [24]. However, accidental scenarios often involve non-homogeneous gas

distribution, and most of them result in deflagration rather than detonation. These factors significantly influence the energy-yielding efficiency and can explain the variation in our findings. The same procedures followed to get the primary estimation of equivalent TNT mass in the following two scenarios, but the final energy efficiency factors were obtained when the numerical outcome was comparable to the test results. It is important to note that the mesh size and boundary conditions for all three methods (CESE-Chemistry coupling, high-pressure, and TNT equivalent) were identical.

2.5.2. Case 2 - Hydrogen detonation in open-air space with blast wall

A H_2-air detonation experiment was carried out by Nozu et al. [47] in open-air space with a blast wall. As shown in Figure 6, the explosion source was a 5.27 m^3 H_2-air mixture which contained 30% H_2 and 70% air. A reinforced concrete wall, with dimensions of 2 m tall, 10 m long and 0.15 m thick, and a compressive strength of 48 MPa, stands 4 m away from the explosion source. A 10 g of C-4 high explosive was placed at the bottom centre of the explosion source to trigger a direct detonation.

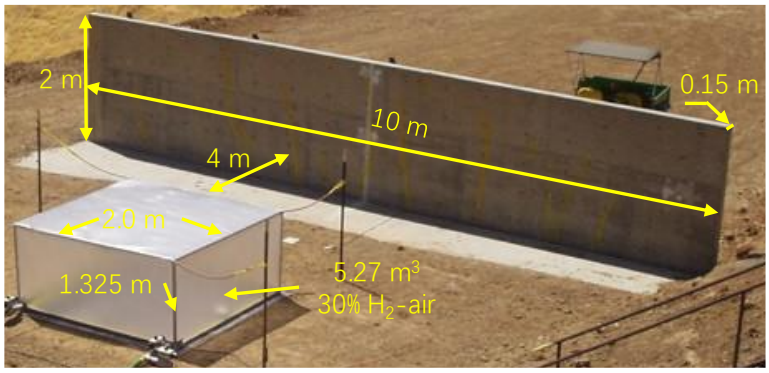

Figure 6 The experimental setup [47]

Figure 7 presents the locations of pressure and displacement sensors. Three pressure sensors (P_1, P_8, P_9) were located along the ground surface in front of and behind the concrete wall, and six pressure sensors were installed on the surface of the wall (P_2, P_3 and P_4 at front, and P_5, P_6 and P_7 at rear). Six displacement sensors were installed at the back of the wall of which

three of them (D_1, D_3 and D_5) were at the middle height of the wall and another three (D_2, D_4 and D_6) at the top of the wall.

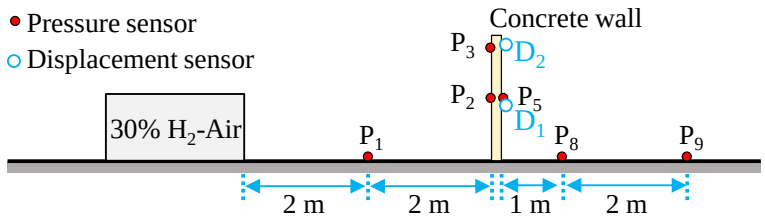

(a) Pressure and displacement positions along the ground

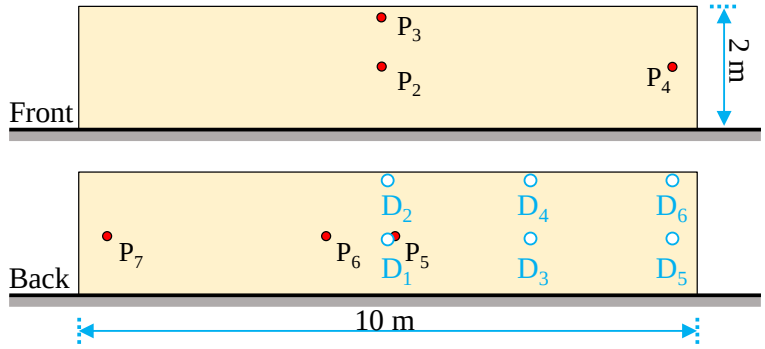

(b) Pressure and displacement positions on the concrete surface

Figure 7 The distribution of sensors [47]

As shown in Figure 8, a half model was numerically established because of the symmetric experimental scenario. The computational domain has dimensions of 12 m long, 8 m wide and 5 m high. The fluid mesh size is 15 mm between the H_2-air mixture and the location 0.5 m after the back of the blast mitigation wall. Other fluid meshed were stretched with an increment rate of 10% until they reached the boundary. The structure meshes were identical and had the sizes of 30 mm. The total number of elements is around 2600×10^4. The bottom of the blast mitigation wall was totally constrained, while a symmetric boundary is applied to its symmetric surface. For the fluid boundary, faces ①, ②, ③ and ⑥ were nonreflective boundary, and face ④ was reflective boundary, and the rest one is symmetric boundary. The material model of blast wall concrete is *MAT_CSCM_CONCRETE with a compressive strength of 48 MPa and a density of 2400 kg/m^3. The strain rate effects were considered for concrete [51]. The material model for reinforcement bar is

*MAT_PIECEWISE_LINEAR_PLASTICITY. Two layers of rebars were modelled as beams with 10 mm diameter and distance of 200 mm.

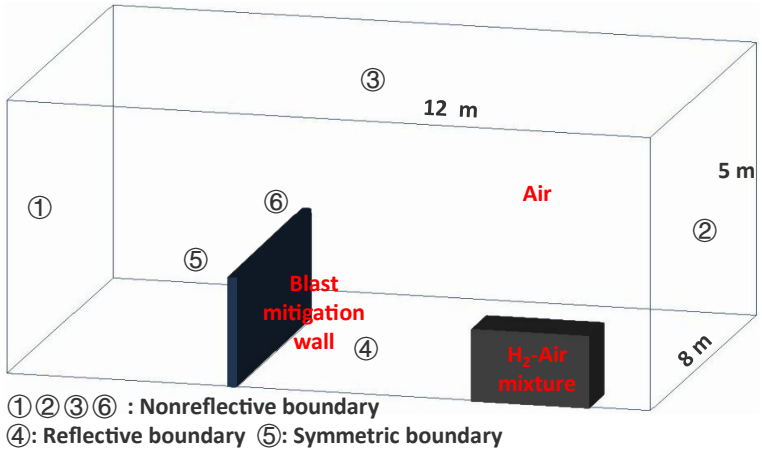

Figure 8 The geometry model and boundary conditions

In the numerical model the TNT equivalent method model, the energy efficiency factor was adjusted to 1, and the equivalent TNT mass was 3.4 kg. Other aspects of the model, such as the mesh size and boundary conditions, remained the same as those used in CESE-chemistry coupling method.

2.5.3. Case 3 – Hydrogen detonation in semi-confined space

Figure 9 illustrates the setup for H_2 detonation tests conducted by Musechke et al. [52]. These tests were carried out in a steel chamber with internal dimensions of 1.8 m × 1.8 m × 1.8 m. The front face of the chamber was open to air, and there was a partial wall extended from the ceiling measuring 0.61 m in length. Plastic bags were used to contain the hydrogen-air mixture, which comprised 30% (vol) hydrogen. In this study, efforts were made to simulate the hydrogen detonation process in two specific tests, namely tests 1-1 and 1-19. As shown in Figure 10, for test 1-1, the H_2-air mixture, with a volume of 0.283 m^3, was located at the bottom center of the chamber. The fuel mixture was detonated at the center of the plastic bag using 6 g of C4 high explosive. For the test 1-19, the volume of H_2-air mixture was 2.83 m^3 which was located at the center of the chamber. The detonation was triggered at the top center

of the fuel. Pressure sensors were installed inside the chamber wall, and their locations are illustrated in Figure 11.

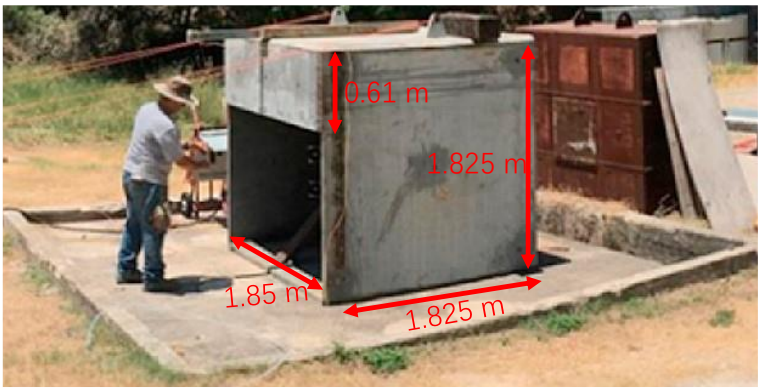

Figure 9 Site image of the test[52]

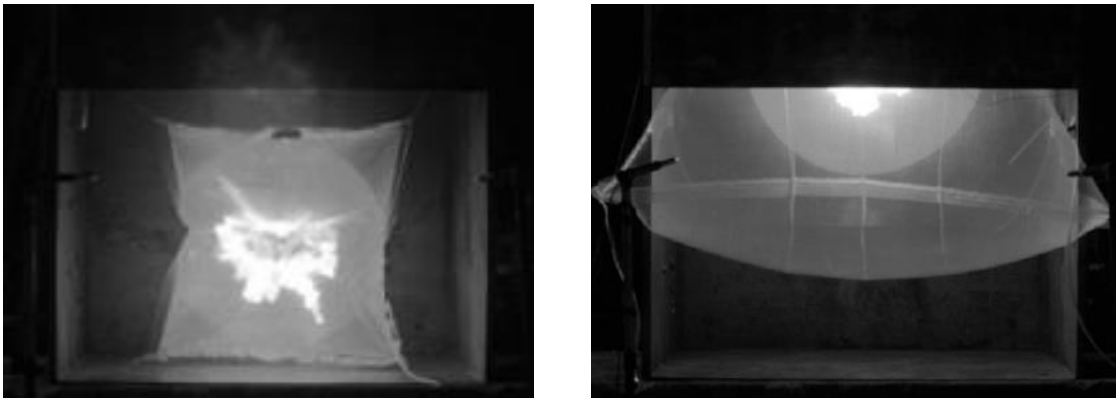

(a) Site image for Test 1-1 **(b) Site image for Test 1-19**

Figure 10 Site images for the hydrogen-air detonation in chamber. The plastic bags have irregular shapes, which were simplified to cubic in numerical model [52]

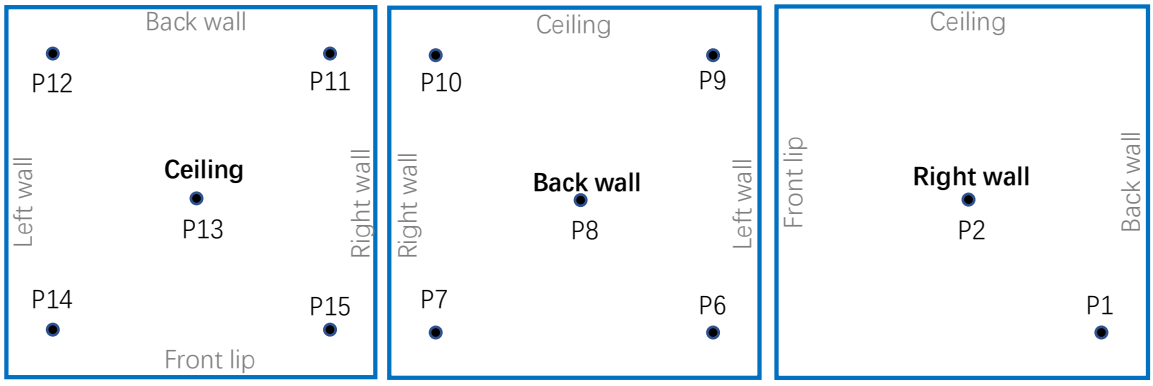

Figure 11 The pressure sensors inside the chamber[52]

As shown in Figure 12, owing to the symmetric nature of the problem, only half of the scenario was modelled. In the numerical model, the shape of the fuel bag was simplified as cubic. The dimensions of the H_2-air region for tests 1-1 and 1-19 were 1.12 m × 1.12 m × 0.23 m and 1.8 m × 1.8 m × 0.87 m, respectively. To ensure mesh size independence, mesh

refinement studies were conducted. For test 1-1, the mesh size within the chamber was set to 6.25 mm, resulting in approximately 1600 × 10^4 elements. For test 1-19, the mesh size within the chamber was set to 5 mm, leading to approximately 3400 × 10^4 elements. The number of elements was optimized to achieve accurate results without unnecessary computational cost. The outer meshes were expanded with an increment rate of 10% until they reached boundaries. The chamber wall was modelled as rigid, with all degrees of freedom constrained to simulate a fixed boundary condition. The floor was set as reflective boundary, and the symmetric face and outer faces were designated as symmetric and nonreflective boundaries, respectively. Because of the symmetric nature of the numerical model, only a portion of the pressure data from specific sensors (P1, P2, P7, P8, P10, P11, P13 and P15) was compared against the corresponding experimental results.

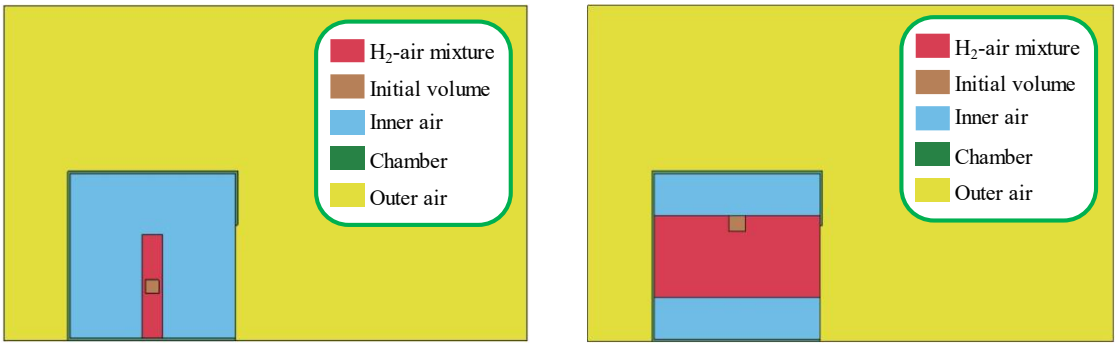

(a) Geometry model for Test 1-1 **(b) Geometry model for Test 1-19**

Figure 12 Geometry models established for CESE-chemistry coupling method

In the numerical model using the TNT equivalent method, the equivalent TNT mass for tests 1-1 and 1-19 were 0.181 kg and 1.81 kg, respectively. This determination was achieved by setting the energy efficiency factor to 1. Other aspects of the model, such as the mesh size and boundary conditions, remained the same as those used in CESE-chemistry coupling method.

3. Results and discussion

All these simulations in this study were performed on the high-performance cluster provided by the University of Technology Sydney. Each node in the cluster is equipped with 64 cores (2 × AMD EPYC 7532, base frequency 2.40 GHz, max turbo frequency 3.33 GHz) and 1024

GB (3200 MHz ECC DDR4, eight channel) of memory. This high-performance computing infrastructure allowed for efficient execution of the simulations and handling of the computational requirements of the study. The commercial code, LS-DYNA R 13.1.1, was utilised to perform the numerical simulation. In the following section, a comparison was made between the accuracy and computational efficiency of the three numerical models used in the study.

3.1. Case 1 - Open-air space

Figure 13 displays the scaled peak pressure over scaled distance, indicating that the peak pressure magnitudes predicted by the three methods are closely aligned, with differences remaining within 30% as compared to the experimental results at a scaled distance of 1.77 $m/kg^{1/3}$ or greater. This finding indicates that all the three methods have comparable and good performance when the scaled distance is sufficiently large (for reference, $Z > 1.18$ $m/kg^{1/3}$ can be considered as the far-field according to the American Society of Civil Engineers [53]). At a scaled distance of 1.33 $m/kg^{1/3}$, the numerical results from the CESE-chemistry coupling method overestimated by 40%. High-pressure volume method had discrepancies of 1%. However, the peak pressure calculated by TNT equivalent method exhibited a remarkable bias from the experimental results, overestimating the value by 89%. As the scaled distance decreased to 0.89 $m/kg^{1/3}$, the CESE-chemistry coupling method underestimated the peak pressure by 17%, while the TNT equivalent method overestimated the pressure by 28%, and the high-pressure volume method underestimated the pressure by 46%. It should be noted that the measuring point was within the H_2-air mixture when scaled distance was 0.89 $m/kg^{1/3}$. Therefore, the peak pressure for the high-pressure volume method was the initial pressure. According to Equation 5, the initial pressure for high-pressure volume method was determined by the properties of combustion production and the combustion energy, which was fixed at 0.61 MPa for the 30% H_2-air mixture detonation. Therefore, it was inevitable that the

high- pressure volume method will underestimate the peak pressure if it was used to predict the pressure within or near the fuel cloud boundary.

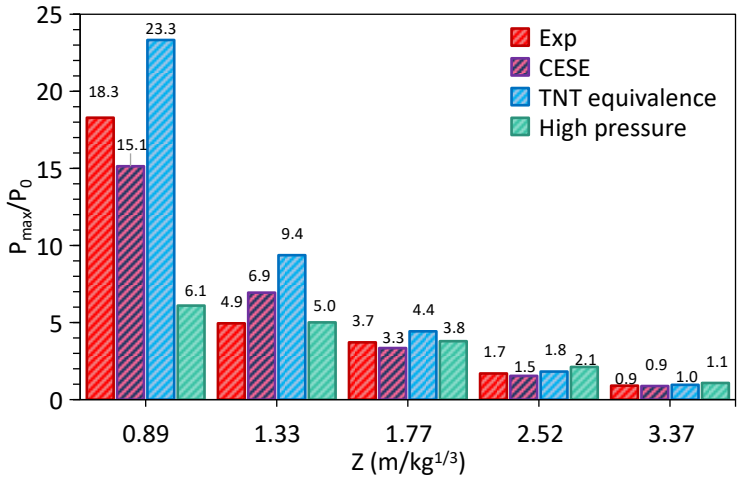

Figure 13 Scaled peak pressure over scaled distance [49]

Figure 14 and Figure 15 represent the pressure-history and impulse-history profiles, respectively. It is evident that all three numerical methods captured both the pressure peak and the pressure variation trend, exhibiting good agreement with the experimental results. The CESE-chemistry coupling method produced a longer positive duration, which matched the experimental behavior. This can be attributed to the fact that the CESE-chemistry coupling method considered the real hydrogen combustion process, which has a detonation velocity of 1971 m/s [13]. In contrast, the TNT equivalent method mimics the combustion process procedure in a much faster progress and much smaller size of fuel, with a combustion velocity of 6930 m/s, and the high-pressure method assumed the combustion process was completed at the start of simulation. The longer positive duration from the CESE-chemistry coupling method led to a better prediction of the impulse-history, with a discrepancy of only 11%. On the other hand, the TNT equivalent method and high-pressure volume method both underestimated the peak impulse, with discrepancies of 38% and 29%, respectively.

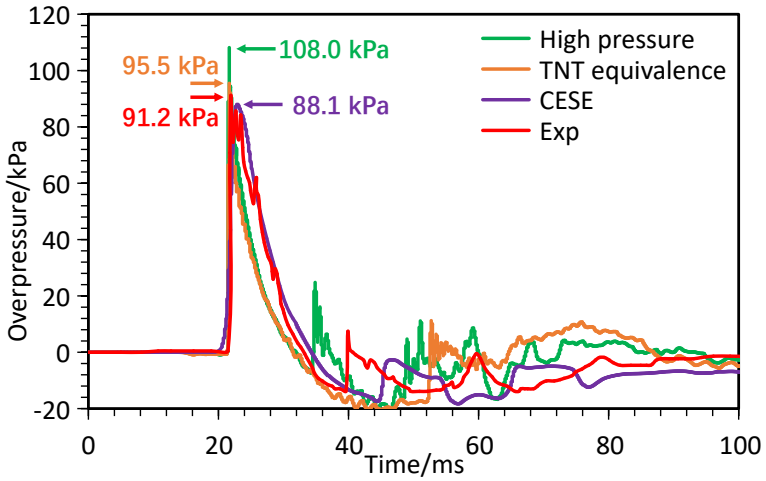

Figure 14 Pressure-history profile at 15.61 m (Z=3.37 m/kg$^{1/3}$) from the ignition point [49]

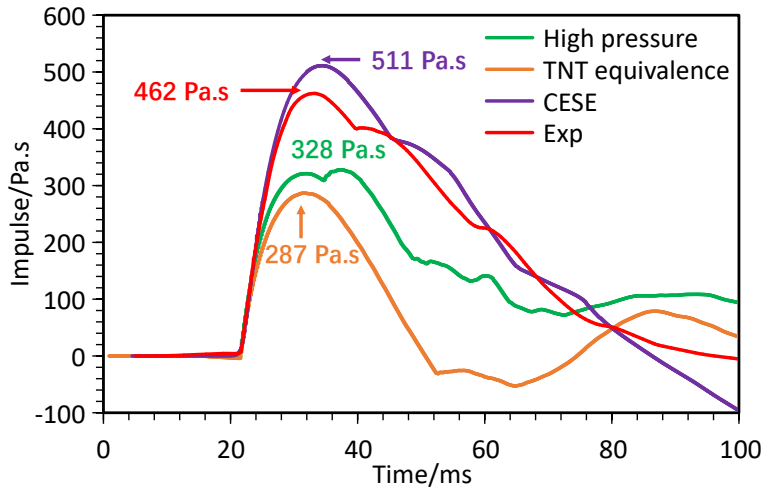

Figure 15 Impulse-history profile at 15.61 m (Z=3.37 m/kg$^{1/3}$) from the ignition point [49]

Figure 16 illustrates the computational efficiency comparison of the three numerical models. It is evident that the TNT equivalent method and high-pressure method required a similar amount of time to complete the numerical simulations. However, the CESE-chemistry method took more than 17 times longer to finish the simulation. A closer look at Figure 16 (b) reveals that the chemistry solver accounted for almost 70% of the computation time in the CESE-chemistry coupling method. This substantial contribution from the chemistry solver was the primary reason for the extended computation time of the CESE-chemistry method as compared to the other two methods.

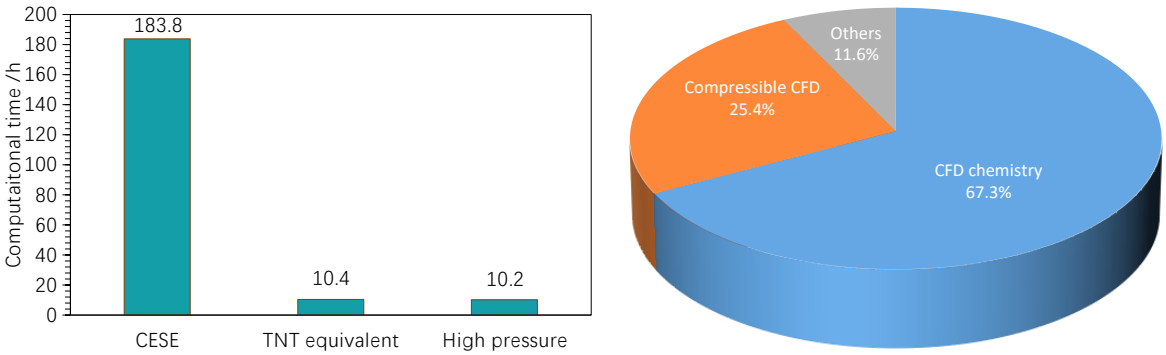

(a) Computational hour comparison among the three methods

(b) The percentage of computational hour spent in difference process for CESE-chemistry coupling method

Figure 16 Computational efficiency comparison of the three numerical models

3.2. Case 2 - Open-air space with blast wall

Figure 17 depicts the scaled peak pressure comparison at various scaled distances from the ignition point. The peak pressures obtained from all the three methods demonstrate good agreement with the data from the experiment, with bias ranging from -12% to 6% from CESE-chemistry coupling method, 0.3% to 32% for TNT equivalent method, and 14% to 45% for high-pressure volume method in the front of the blast wall ($Z \leq 4.72$ m/kg$^{1/3}$). The presence of blast mitigation wall significantly reduced the pressure, as evidenced by the dramatic drop in peak pressure after the wall (Z=3.40 m/kg$^{1/3}$ VS Z=4.72 m/kg$^{1/3}$), which was reproduced well by the three methods. The magnitudes of peak pressure also indicated that the CESE-chemistry coupling method tends to slightly underestimate the peak pressure, while the other two methods tend to overestimate the peak pressure. However, overall, as previously mentioned, all the three methods performed well if the scaled distance is large enough ($Z \geq 2$ m/kg$^{1/3}$ in this case).

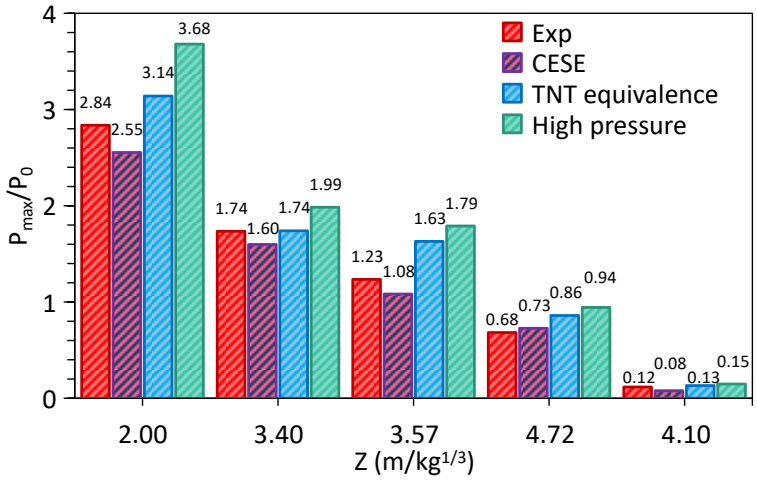

Figure 17 Scaled peak pressure over scaled distance [47]

Figure 18 illustrates the pressure-time history on the front and rear surface of the blast wall. It is evident that the pressure peak and trend on the front surface of the blast wall were captured quite well by the three methods, and the relative differences of peak pressure were less than 10% for CESE-chemistry coupling method, and within 26% and 40% for TNT equivalent method and high-pressure volume method, respectively. The pressure history on the rear surface of the wall was slightly less accurate, but the main trend, such as the dominant pressure peaks and the pressure duration, were reproduced satisfactorily. The peak pressure on the rear surface had a relative error of less than 50%. Considering the inherent uncertainty in blast tests [18] and the relatively lower magnitudes of pressure on the rear surface of the blast wall, these discrepancies are considered acceptable.

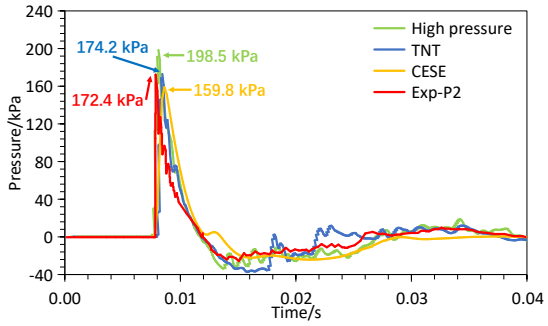

(a) The pressure-time history at the centre of front surface

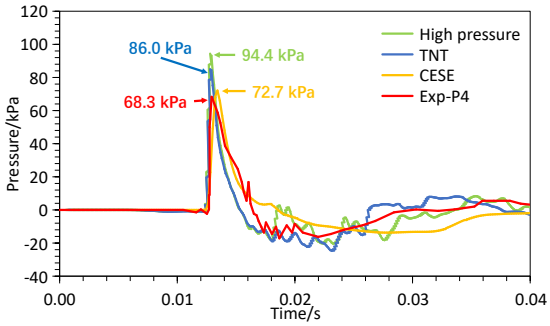

(b) The pressure-time history at the right hand of front surface

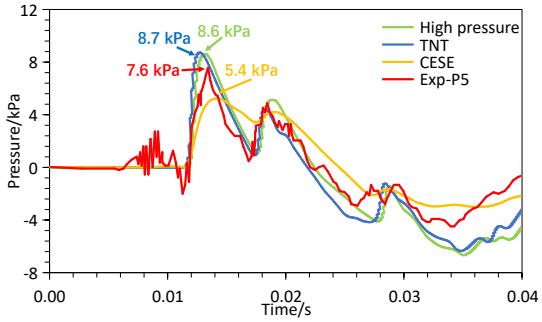

(c) The pressure-time history at the centre of back surface

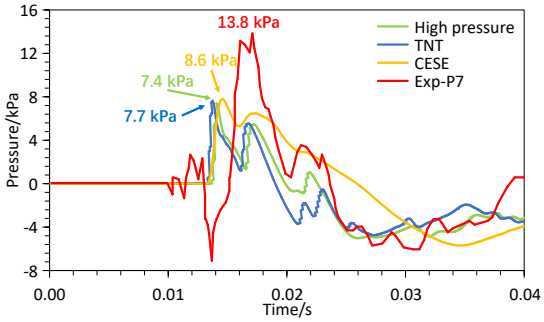

(d) The pressure-time history at the right hand of back surface

Figure 18 The pressure-time history at the front and back of the blast mitigation wall [47]

The impulse-time comparison on the front and back of the wall is illustrated in Figure 19. Again, the basic trend of impulse was captured well by the three methods. The peak impulses from the CESE-chemistry coupling method were consistently higher than the experimental ones. By comparison, the TNT equivalent method and high-pressure volume method underestimated the peak impulse in some cases.

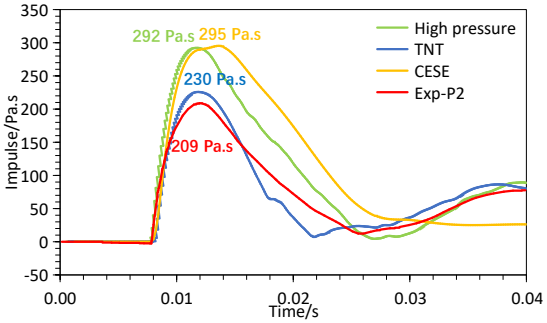

(a) The impulse-time history at the centre of front surface

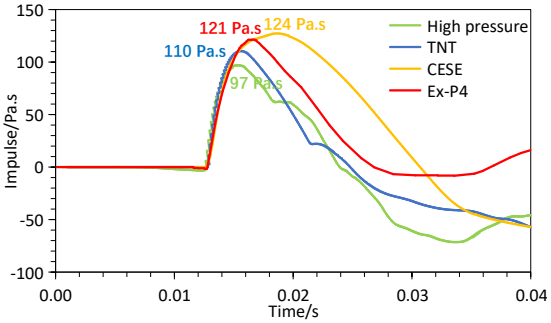

(b) The impulse-time history at the right hand of front surface

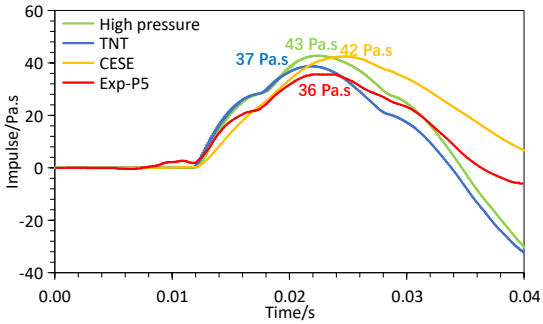

(c) The impulse-time history at the centre of back surface

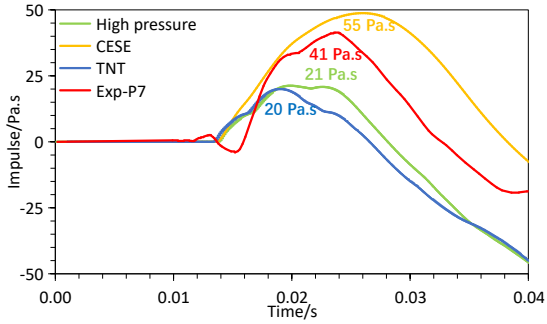

(d) The impulse-time history at the right hand of back surface

Figure 19 The impulse-time history at the front and back of the blast mitigation wall [47]

Figure 20 illustrates a comparison of displacement over time, revealing that all the three methods successfully captured the basic trend of displacement variation. However, there are notable differences in their performance: (1) the CESE-chemistry coupling method

consistently yielded slightly higher predictions within a variation range of 10% to 24.4%. (2) The other two methods may significantly underestimate the structural response as evidenced by a discrepancy of -35% for the TNT equivalent method at the centre of the blast wall, and a difference of -27% for the high-pressure method at the top right corner of blast wall. There disparities can be attributed to the underlying assumptions and models used in each method: the CESE-chemistry coupling method considers real chemical reactions, leading to longer pressure durations and, consequently, a more conservative predictions of structural response. In contrast, the TNT equivalent method and high-pressure volume method do not account for chemical reactions, leading to instant pressure rises and lower structural responses.

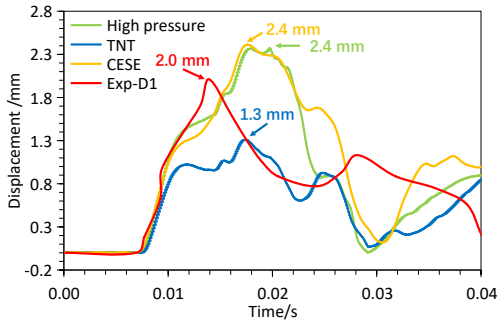

(a) The displacement-time history at the centre of blast wall

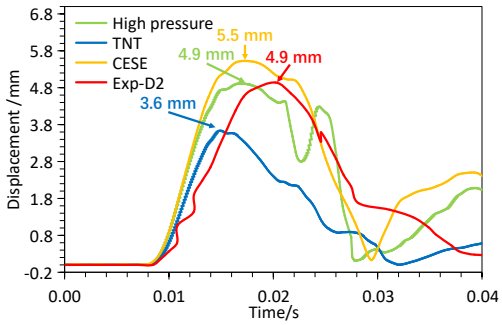

(b) The displacement-time history at the upper centre of blast wall

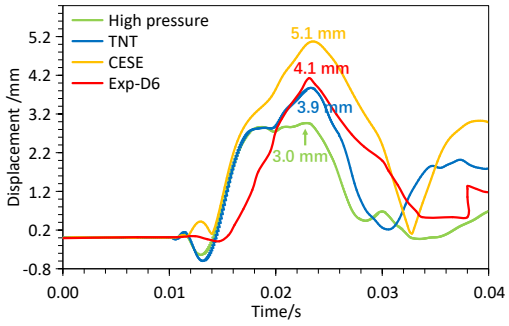

(c) The displacement-time history at the top right corner of blast wall

Figure 20 The displacement-time history at the blast mitigation wall [47]

It is essential to emphasize that the literature only provided the compressive strength of the concrete blast wall [47], with other material characteristics (such as density, Young's modulus, Poisson's ratio, and strain rate effect) assumed or automatically generated by the LS-DYNA code. Similarly, a generic reinforcement in the wall and made it constant in each modelling trial was assumed. Nevertheless, the comparison shown in Figure 20 revealed accuracy of

each modelling method against the test, and demonstrated the bias tendencies of the three methods in predicting the dynamic behavior of structures exposed to hydrogen detonation.

Figure 21 presents the computational efficiency comparison of the three numerical models. As observed before, the CESE-chemistry method required significantly more computational time (approximately 15 times) to complete the simulation in comparison with the other two methods. Moreover, 70% of CPU time was consumed to solve the chemical reaction using CESE-chemistry method.

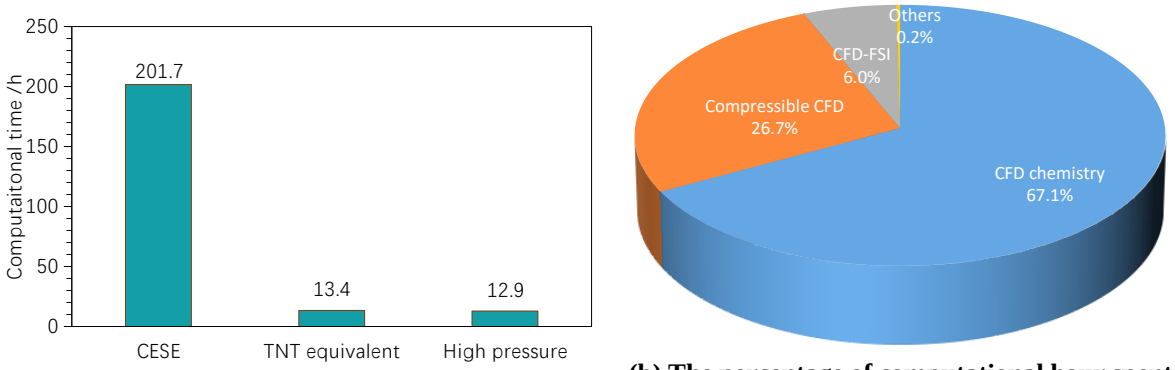

(a) Computational hour comparison among the three methods

(b) The percentage of computational hour spent in difference process for CESE-chemistry coupling method

Figure 21 Computational efficiency comparison of the three numerical models

3.3. Case 3 - Semi-confined space

As shown in Figure 22 and Figure 23, the extra confinement resulting from the steel chamber caused the waveform in the semi-confined space to be significantly more complex in contrast to an open-air detonation scenario. The presence of chamber walls led to multiple pressure wave reflections, resulting in multiple peaks in the pressure-time history. In the case of test 1-1 (1.7 m/kg$^{1/3}$≤Z≤2.66 m/kg$^{1/3}$), all the three methods produced comparable results with the same mesh resolution. The dominant pressure peaks and the multiple reflections were captured quite well, despite minor discrepancies among the peak pressures and pressure variation trend. These differences in the numerical results could arise from various sources, including either the modelling methods themselves or the simplifications made during the

modelling process. For example, the shape of H_2-air mixture was simplified as cuboid, and the plastic bag containing the fuel was ignored, which could affect the accuracy of the numerical model.

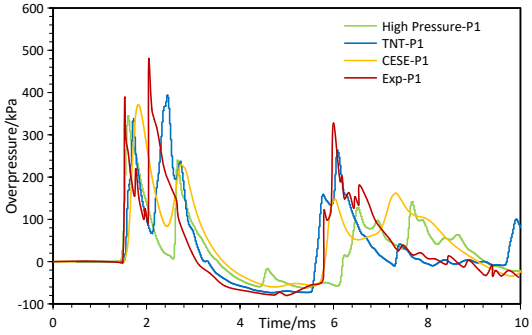

(a) The pressure-time history for P1 (Z=1.97 m/kg$^{1/3}$)

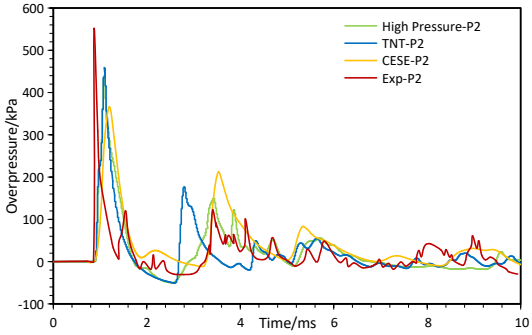

(b) The pressure-time history for P2 (Z=1.70 m/kg$^{1/3}$)

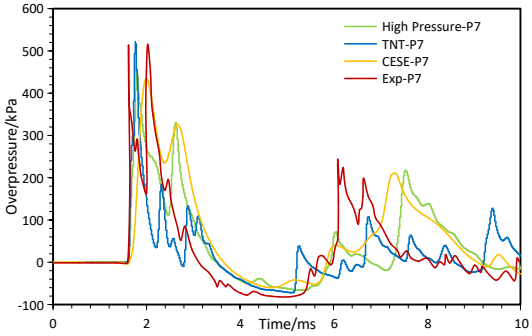

(c) The pressure-time history for P7 (Z=1.97 m/kg$^{1/3}$)

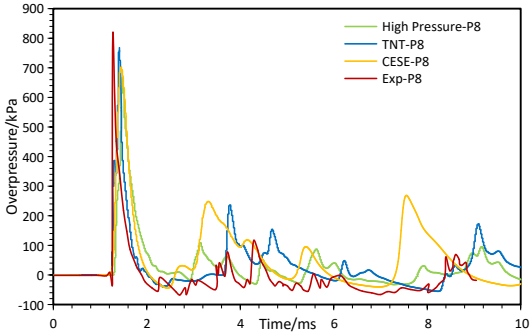

(d) The pressure-time history for P8 (Z=1.70 m/kg$^{1/3}$)

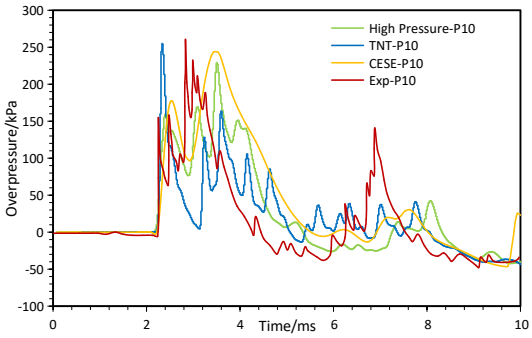

(e) The pressure-time history for P10 (Z=2.53 m/kg$^{1/3}$)

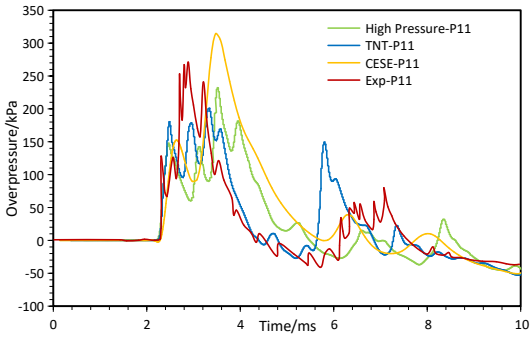

(f) The pressure-time history for P11 (Z=2.66 m/kg$^{1/3}$)

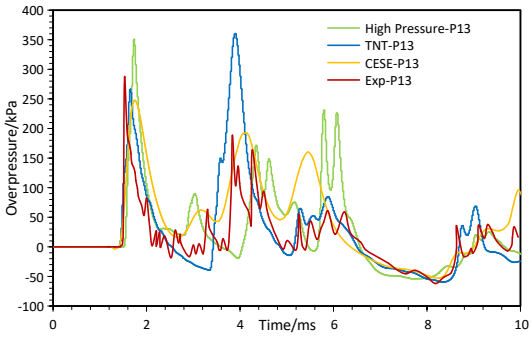

(g) The pressure-time history for P13 (Z=2.19 m/kg$^{1/3}$)

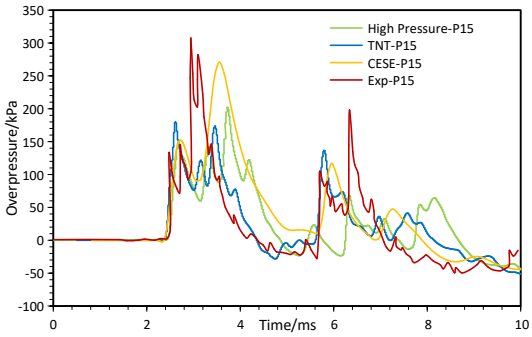

(h) The pressure-time history for P15 (Z=2.66 m/kg$^{1/3}$)

Figure 22 The pressure-time history for test 1-1[52]

In the case of test 1-19, where the scaled distances were much closer, the differences among the three methods became more pronounced. As shown in Figure 23, the TNT equivalent method and CESE-chemistry coupling method demonstrated reasonable accuracy when the scaled distance was 0.79 m/kg$^{1/3}$. In contrast, high-pressure volume method failed to produce the multiple reflected waves of pressure, and the magnitudes of peak pressures were notably lower as compared to the results from the other two methods.

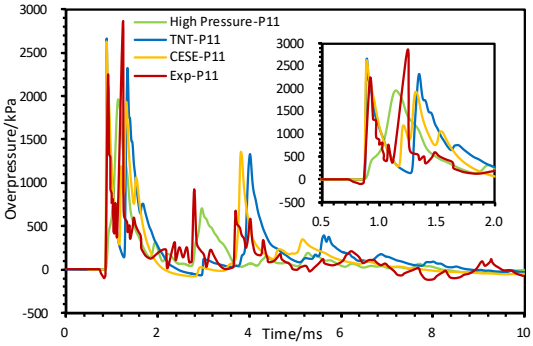

(a) The pressure-time history for P11 (Z=0.79 m/kg$^{1/3}$)

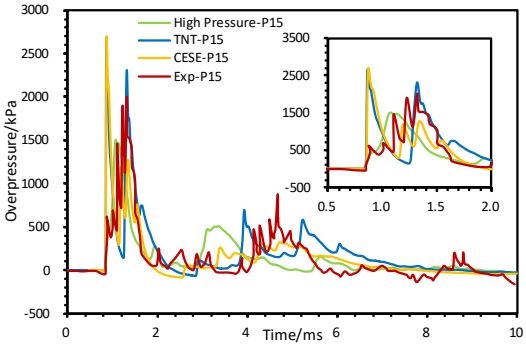

(b) The pressure-time history for P15 (Z=0.79 m/kg$^{1/3}$)

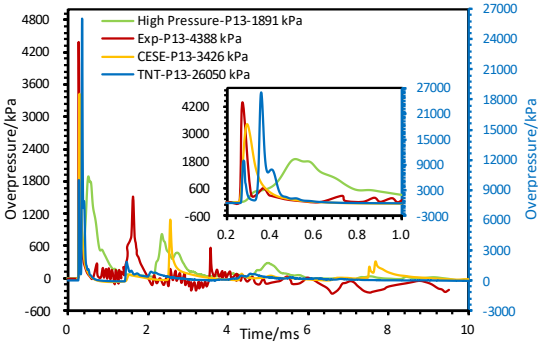

(c) The pressure-time history for P13 (Z=0.37 m/kg$^{1/3}$)

Figure 23 The pressure-time history for test 1-19 [52]

When the scaled distance was close to 0.37 m/kg$^{1/3}$, the discrepancies among the methods became even more notable. Only the CESE-chemistry method maintained reasonable accuracy, underestimating the peak pressure by 22%. On the other hand, the high-pressure volume method underestimated the peak pressure by 57% with longer duration, and the TNT equivalent method significantly overestimated the peak pressure by 494%. These results indicate that only the CESE-chemistry coupling method can produce reasonable prediction when the scaled distance is close. This can be attributed to the fact that the CESE-chemistry coupling method considers the real chemistry process, while the high-pressure volume method inherently underestimates the peak pressure near the fuel cloud. Additionally, as the TNT is a solid charge, it produces significantly higher pressure in near-field explosion because of its intrinsic properties.

Figure 24 presents the computational efficiency comparison among the three numerical methods. Consistent with previous case studies, the CESE-chemistry coupling method required approximately 16 times more CPU time to complete the simulation as compared to the other two methods. Moreover, nearly 60% of the computational time was utilized to solve the chemical reactions, highlighting the significant computational cost associated with considering the detailed chemistry and combustion processes.

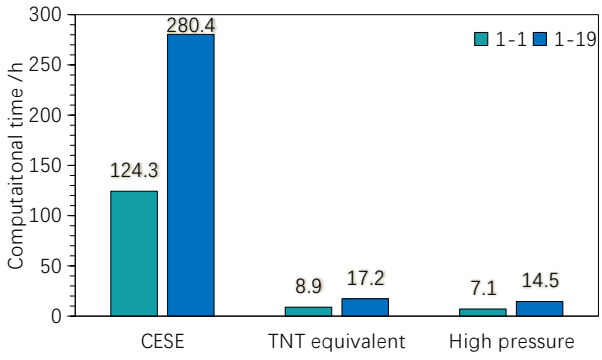

(a) Computational hour comparison among the three methods

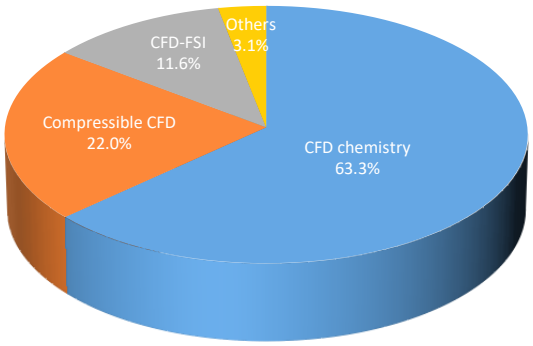

(b) The percentage of computational hour spent in difference process for CESE-chemistry coupling method among the three methods (test 1-19)

Figure 24 Computational efficiency comparison of the three numerical models

4. Conclusion

This study conducted a comprehensive assessment of the accuracy and effectiveness of three distinct methods for predicting hydrogen detonation loads. These methods include the novel CESE-chemistry coupling method, the conventional TNT equivalent method and the high-pressure volume method. The CESE-chemistry coupling method incorporates chemical kinetics within a compressible flow framework and is fully integrated with the structural solver in LS-DYNA. In contrast, the other two methods rely on energy equivalence principles and do not account for chemical reactions. The accuracy was evaluated against the experimental data from three typical scenarios: open-air space, open-air space with a blast wall, and semi-confined space, while the effectiveness was determined by comparing the computational time.

The results revealed that all three methods produced reasonably accurate peak overpressure predictions in large scaled distances ($\geqslant$0.79 m/kg$^{1/3}$). However, the CESE-chemistry coupling method outperformed the others in capturing pressure duration and structural response due to its incorporation of real chemical kinetics, offering more accurate overpressure derivation. As scaled distances decreased to 0.37 m/kg$^{1/3}$, the CESE-chemistry coupling method demonstrated superior accuracy in modelling pressure wave, while the TNT equivalent method tended to overestimate of the peak pressures. On the other hand, the high-pressure volume method underestimated the peak pressure within or near the H_2-air cloud.

However, CESE-chemistry coupling method required significantly higher computational time, approximately 15 to 20 times more than the other two methods. A substantial portion of this time (60% to 70%) was consumed by solving chemical reactions, so simplifying the chemical kinetics could substantially reduce computational time, as the time required for the Chemistry

solver is directly proportional to the square of the number of species in the reaction model. The TNT equivalent method and high-pressure volume method emerged as more computationally efficient alternatives, striking a balance between accuracy and computational speed. Notably, the energy efficiency factor for the TNT equivalent method is notably larger than commonly thought (0.01-0.1) in hydrogen detonation, where 0.51 was chosen for the 300 m^3 hydrogen detonation case, and 1.0 was chosen for the other smaller scale cases.

In conclusion, for scenarios involving close scaled distances, the CESE-chemistry coupling method may be preferred. Conversely, for simulations emphasizing computational efficiency and featuring large scaled distances, the TNT equivalent method or high-pressure volume method may serve as more suitable options.

5. Acknowledgement

This work was supported by the Australia Research Council under ARC Discovery Project DP210101100.

6. Declaration of Generative AI and AI-assisted technologies in the writing process

Statement: During the preparation of this work the authors used ChatGPT, an AI language model in order to improve the readability and language of this work. After using this tool, the authors reviewed and edited the content as needed and take full responsibility for the content of the publication.

7. References

[1]. Hydrogen scaling up: a sustainable pathway for the global energy transition. 2017, Hydrogen Council.

[2]. Hydrogen Strategy-Enabling a Low-Carbon Economy. 2020, United States Department of Energy: Washington, DC, the United States.

[3]. White Paper 2020 on China's Hydrogen Energy and Fuel Cell Industry. 2019, China Hydrogen Alliance: China.

[4]. Hydrogen Roadmap Europe: Fuel Cells and Hydrogen 2 Joint Undertaking. 2019, Hydrogen Europe.

[5]. Hydrogen strategy for Canada. 2020, Natural Resources Canada.

[6]. The national hydrogen strategy. 2020, Federal Ministry for Economic Affairs and Energy: Berlin, Germany.

[7]. Energy Strategy to 2035. 2020, Government of the Russian Federation.

[8]. Japan: Basic Hydrogen Strategy. 2017, Ministerial Council On Renewable Energy.

[9]. Australia's National Hydrogen Strategy. 2019, Council of Australian Governments Energy Council: Australia.

[10]. UK Hydrogen Strategy. 2021, the Secretary of State for Business, Energy & Industrial Strategy.

[11]. National strategy of green hydrogen. 2020, Department of Energy.

[12]. Kim, S., et al., Behavior of Barrier Wall under Hydrogen Storage Tank Explosion with Simulation and TNT Equivalent Weight Method. Applied Sciences, 2023. 13(6): p. 3744.

[13]. Bjerketvedt, D., J.R. Bakke and K. van Wingerden, Gas explosion handbook. Journal of hazardous materials, 1997. 52(1): p. 1-150.

[14]. Hu, Q., X. Zhang and H. Hao, A review of hydrogen-air cloud explosions: The fundamentals, overpressure prediction methods, and influencing factors. International Journal of Hydrogen Energy, 2023.

[15]. Wei, R., et al., A bibliometric study on research trends in hydrogen safety. Process Safety and Environmental Protection, 2022. 159: p. 1064-1081.

[16]. Hao, H., et al., Review of the current practices in blast-resistant analysis and design of concrete structures. Advances in Structural Engineering, 2016. 19(8): p. 1193-1223.

[17]. Zhang, K., et al., Effect of hydrogen concentration on the vented explosion of hydrogen–air mixtures in a 5-m-long duct. Process Safety and Environmental Protection, 2022. 162: p. 978-986.

[18]. Chen, D., et al., A numerical study of gas explosion with progressive venting in a utility tunnel. Process Safety and Environmental Protection, 2022. 162: p. 1124-1138.

[19]. van den Berg, A.C., The multi-energy method: A framework for vapour cloud explosion blast prediction. Journal of Hazardous Materials, 1985. 12(1): p. 1-10.

[20]. López, E., et al., Analysis of high-pressure hydrogen and natural gas cylinders explosions through TNT equivalent method, in Proceeding Hyceltec 2015. Iberian symposium on hydrogen, fuel cells and advanced batteries. 2015.

[21]. Guo, Y., et al., Numerical investigation of surface conduit parallel gas pipeline explosive based on the TNT equivalent weight method. Journal of Loss Prevention in the Process Industries, 2016. 44: p. 360-368.

[22]. Zhang, B.Y., H.H. Li and W. Wang, Numerical study of dynamic response and failure analysis of spherical storage tanks under external blast loading. Journal of Loss Prevention in the Process Industries, 2015. 34: p. 209-217.

[23]. Zhang, Q., et al., Risk evaluation and analysis of a gas tank explosion based on a vapor cloud explosion model: A case study. Engineering Failure Analysis, 2019. 101: p. 22-35.

[24]. Van den Berg, A.C. and A. Lannoy, Methods for vapour cloud explosion blast modelling. Journal of Hazardous Materials, 1993. 34(2): p. 151-171.

[25]. Jiang, H., et al., Numerical investigation and analysis of indoor gas explosion: A case study of "6·13" major gas explosion accident in Hubei Province, China. Journal of Loss Prevention in the Process Industries, 2023. 83: p. 105045.

[26]. Zhang, B., et al., Pressure characteristics and dynamic response of coal mine refuge chamber with underground gas explosion. Journal of Loss Prevention in the Process Industries, 2014. 30: p. 37-46.

[27]. Machniewski, P. and E. Molga, CFD analysis of large-scale hydrogen detonation and blast wave overpressure in partially confined spaces. Process Safety and Environmental Protection, 2022. 158: p. 537-546.

[28]. Yáñez, J., et al., A comparison exercise on the CFD detonation simulation in large-scale confined volumes. International Journal of Hydrogen Energy, 2011. 36(3): p. 2613-2619.

[29]. Heidari, A., et al., Numerical simulation of large scale hydrogen detonation. International Journal of Hydrogen Energy, 2011. 36(3): p. 2538-2544.

[30]. Kim, D. and J. Kim, Numerical method to simulate detonative combustion of hydrogen-air mixture in a containment. Engineering applications of computational fluid mechanics, 2019. 13: p. 938-953.

[31]. Malik, K., et al., Numerical and experimental investigation of H2-air and H2O2 detonation parameters in a 9 m long tube, introduction of a new detonation model. International Journal of Hydrogen Energy, 2019. 44(17): p. 8743-8750.

[32]. Zhang, S., et al., Numerical simulation on methane-hydrogen explosion in gas compartment in utility tunnel. Process Safety and Environmental Protection, 2020. 140: p. 100-110.

[33]. Li, Y., et al., Safety analysis of hydrogen leakage accident with a mobile hydrogen refueling station. Process Safety and Environmental Protection, 2023. 171: p. 619-629.

[34]. Zhang, Z., G. Cook and Jr. K. Im, Overview of the CESE Compressible Fluid and FSI Solvers, in 16th International LS-DYNA Users Conference. 2020: Virtual Event.

[35]. Rokhy, H. and H. Soury, Investigation of the confinement effects on the blast wave propagated from gas mixture detonation utilizing the CESE method with finite rate chemistry model. Combustion Science and Technology, 2021.

[36]. Chang, S., The Method of Space-Time Conservation Element and Solution Element—A New Approach for Solving the Navier-Stokes and Euler Equations. Journal of computational physics, 1995. 119(2): p. 295-324.

[37]. Cook, G., Z. Zhang and K. Im, Applications of the CESE method in LS-DYNA, in 21st AIAA Computational Fluid Dynamics Conference. 2013: San Diego, CA.

[38]. Rokhy, H. and H. Soury, Fluid structure interaction with a finite rate chemistry model for simulation of gaseous detonation metal-forming. International Journal of Hydrogen Energy, 2019. 44(41): p. 23289-23302.

[39]. Rokhy, H. and T.M. Mostofi, 3D numerical simulation of the gas detonation forming of aluminum tubes considering fluid-structure interaction and chemical kinetic model. Thin-Walled Structures, 2021. 161: p. 107469.

[40]. Rokhy, H. and T.M. Mostofi, Tracking the explosion characteristics of the hydrogen-air mixture near a concrete barrier wall using CESE IBM FSI solver in LS-DYNA incorporating the reduced chemical kinetic model. International Journal of Impact Engineering, 2023. 172: p. 104401.

[41]. Chen, D., et al., An overpressure-time history model of methane-air explosion in tunnel-shape space. Journal of Loss Prevention in the Process Industries, 2023. 82: p. 105004.

[42]. Liao, K., et al., Parametric Study on Natural Gas Leakage and Diffusion in Tunnels. Journal of Pipeline Systems Engineering and Practice, 2023. 14(2).

[43]. Zettervall, N. and C. Fureby, A Computational Study of Ramjet, Scramjet and Dual-mode Ramjet Combustion in Combustor with a Cavity Flameholder, in 2018 AIAA aerospace sciences meeting. 2018: Kissimmee, Florida. p. 1146.

[44]. Im, K., LNG Combustion using the CESE and Chemistry Solvers in LS-DYNA. 2018.

[45]. LS-DYNA® Keyword User's Manual Volume II. 2021, Livermore Software Technology.

[46]. Souli, M., et al., ALE and Fluid Structure Interaction in LS-DYNA, in 8th International LS-DYNA Conference. 2004: Detroit.

[47]. Nozu, T., et al., Numerical Simulation of Hydrogen Explosion Tests with a Barrier Wall for Blast Mitigation, in Proceedings of the 1st International Conference on Hydrogen Safety. 2005: Pisa, Italy.

[48]. Szwaja, S., Simplified calculation of combustion progress in the IC engine. Teka Commission of Motorization and Power Industry in Agriculture, 2011. 11: p. 386–396.

[49]. GROETHE, M., et al., Large-scale hydrogen deflagrations and detonations. International Journal of Hydrogen Energy, 2007. 32(13): p. 2125-2133.

[50]. UN Saferguard, Kingery-Bulmash Blast Parameter Calculator.

[51]. Novozhilov, Y.V., A.N. Dmitriev and D.S. Mikhaluk, Precise Calibration of the Continuous Surface Cap Model for Concrete Simulation. Buildings, 2022. 12(5): p. 636.

[52]. Mueschke, N.J. and A. Joyce, Measurement of gas detonation blast loads in semiconfined geometry. Journal of Loss Prevention in the Process Industries, 2020. 63: p. 104004.

[53]. Dua, A. and A. Braimah, State-of-the-art in near-field and contact explosion effects on reinforced concrete columns, in 5th International Structural Specialty Conference. 2016, Canadian Society for Civil Engineering: Canada.